Asn249Tyr Substitution at the Coenzyme Binding Domain Activates *Sulfolobus solfataricus* Alcohol Dehydrogenase and Increases Its Thermal Stability†

A. Giordano,‡ R. Cannio,‡,§ F. La Cara,‡ S. Bartolucci,|| M. Rossi,‡,|| and C. A. Raia*,‡

Institute of Protein Biochemistry and Enzymology, CNR, 80125 Naples, Italy, and Department of Organic and Biological Chemistry, University of Naples "Federico II", 80134 Naples, Italy

Received September 28, 1998; Revised Manuscript Received December 21, 1998

ABSTRACT: A mutant of the thermostable NAD^+-dependent homotetrameric alcohol dehydrogenase from *Sulfolobus solfataricus* (SsADH), which has a single substitution, Asn249Tyr, located at the coenzyme binding domain, was obtained by error prone PCR. The mutant enzyme, which was purified from *Escherichia coli* to homogeneous form, exhibits a specific activity that is more than 6-fold greater than that of the wild type enzyme, as measured at 65 °C with benzyl alcohol as the substrate. The oxidation rate of aliphatic alcohols and the reduction rate of aromatic aldehydes were also higher. The dissociation constants for NAD^+ and NADH determined at 25 °C and pH 8.8 were 3 orders of magnitude greater compared to those of the wild type enzyme. It is thought that the higher turnover of the mutant SsADH is due to the faster dissociation of the modified enzyme−coenzyme complex. Spectroscopic studies showed no relevant changes in either secondary or tertiary structure, while analysis with fluorescent probes revealed a significant increase in surface hydrophobicity for the mutant, with respect to that of the wild type molecule. The mutant SsADH displays improved thermal stability, as indicated by the increase in T_m from 90 to 93 °C, which was determined by the apparent transition curves. Kinetic thermal stability studies at pH 9.0 for mutant SsADH showed a marked increase in activation enthalpy compensated by an entropy gain, which resulted in a higher activation barrier against thermal unfolding of the enzyme. Ammonia analysis showed that the Asn249Tyr substitution produced the effect of markedly reducing the extent of deamidation during thermoinactivation, thus suggesting that Asn249 plays a significant role in the mechanism of irreversible thermal denaturation of the archaeal ADH. Furthermore, the decrease in the activating effect by moderate concentrations of denaturants and studies with proteases and chelating agents point to an increase in structural rigidity and a tightening of structural zinc as additional factors responsible for the improved thermal resistance of the mutant enzyme.

Enzymes from thermophilic organisms differ from those of mesophilic organisms in stability and temperature dependence of activity (*1*, *2*). The higher thermal stability of thermophilic enzymes correlates with the higher structural rigidity achieved by the protein molecule to compensate for the increased thermal mobility in its natural environment (*3*, *4*). The limited degree of flexibility in thermophilic enzymes results in reduced catalytic efficiency when compared to that of their mesophilic counterpart at low temperatures (*5*).

Although the mechanism of protein stabilization and predictive structural analysis for strategies for engineering more stable enzymes have been the object of various studies (*6*−*8*), the problem of enhancing the efficiency of enzymes has been approached in specific cases with site directed mutagenesis (*9*−*11*), directed evolution (*12*), or additive addition (*13*). However, the possibility of designing fast enzymes by mutating charged residues on the enzyme surface has been recently discussed, using superoxide dismutase as a model (*14*). Substitutions at and near the active site in yeast and horse liver alcohol dehydrogenase have been introduced to show how they can affect substrate specificity and reactivity (*15*). More specifically, substitutions at the adenine binding site proved to be able to activate the horse liver enzyme (*16*).

Alcohol dehydrogenase from the archaeon *Sulfolobus solfataricus* (SsADH)[1] is a thermophilic NAD^+-dependent homotetrameric enzyme endowed with a broad substrate specificity and stereoselectivity (*17*). The enzyme contains two zinc atoms per subunit. The catalytic zinc is bound to two out of five cysteine residues present per subunit and one histidine residue, while the structural zinc is coordinated to the remaining three cysteines and one glutamate residue.

† This work was in part financed by EC-Project "Extremophiles as Cell Factories" (Contract BIO4-CT96-0488), and A.G. is a recipient of a postdoctoral fellowship.

* To whom correspondence should be addressed: IBPE, CNR, Via G. Marconi 10, 80125 Napoli, Italy. Fax: +39-081-7257240. E-mail: raia@dafne.ibpe.na.cnr.it.

‡ CNR.

§ Present address: Instituto di Scienze dell'Alimentazione, CNR, 83100 Avellino, Italy.

|| University of Naples "Federico II".

[1] Abbreviations: ADH, alcohol dehydrogenase; SsADH, *S. solfataricus* ADH; mSsADH, N249Y SsADH; HLADH, horse liver ADH; YADH, yeast ADH; TBADH, *Thermoanaerobium brockii* ADH; ANS, 8-anilino-1-naphthalene-1-sulfonic acid; PMSF, phenylmethanesulfonyl fluoride; IPTG, isopropyl β-D-thiogalactopyranoside; GdmCl, guanidinium chloride.

10.1021/bi982326e CCC: $18.00
Published on Web 02/19/1999

The sequence of SsADH has been determined by gene and peptide analysis (*18*), while the tetrameric structure has been defined by Cannio et al. (*19*), who have also reported the expression of the SsADH gene in *Escherichia coli*. Crystals of SsADH in the apo and holo forms complexed with NADH have been obtained (*20*). More recently, the effect of microgravity on the growth and twinning of holo SsADH crystals has been investigated (*21*). SsADH has a remarkable stability to heat and against denaturants but shows a lower specific activity when compared to ADH from mesophilic or moderately thermophilic sources, i.e., horse liver (*17*) and *Bacillus stearothermophilus* LLD-R (*22*). However, selective carboxymethylation of Cys38, a ligand of the catalytic zinc in SsADH, results in a more active although less stable enzyme, as recently reported (*23*).

As an alternative approach to improving the SsADH turnover, a random mutagenesis strategy on the coding gene was adopted. This paper describes the isolation of an SsADH mutant (Asn249Tyr), which is more active and stable than the wild type enzyme, as shown by the analysis of the kinetic parameters, kinetics of thermal unfolding, and guanidinium-dependent deactivation. Ammonia analysis shows a marked decrease in the deamidation rate upon the Asn249Tyr substitution. Furthermore, both the decrease in the activating effect by moderate concentrations of denaturants and studies with chelating agents and proteases point to an increase in the structural rigidity and a tightening of structural zinc as additional factors responsible for the improved thermal resistance of the mutant enzyme.

MATERIALS AND METHODS

Chemicals. NAD^+ and NADH were purchased from either Fluka (Buchs) or Applichem (Darmstadt, FRG). DEAE Sepharose Fast Flow and Sephadex G-75 were from Pharmacia. Ampicillin, PMSF, and IPTG were purchased from Sigma Chemical Co. (St. Louis, MO). Protamine sulfate was from Calbiochem. DNase I, grade I, thermolysin, α-chymotrypsin, and glutamate dehydrogenase were from Boehringer Mannheim. Guanidinium chloride was from Pierce. Alcohols and aldehydes were from Fluka and Aldrich. Cyclohexanol-d_{12}, benzyl-d_7 alcohol, 8-anilinonaphthalene-1-sulfonic acid, and pyrazole were from Aldrich. Other chemicals were A grade substances from Sigma or Applichem.

Bacterial Strains, Plasmids, and Enzymes. *E. coli* RB791 (*24*) was used for heterologous gene expression, and TOP10F′ (Invitrogen) was used for plasmid isolation and propagation. Plasmid pGEM5Zf(−) was purchased from Promega and PTrc99A from Pharmacia. Restriction and modification enzymes were from Boehringer Mannheim. The Sequenase kit, as well as radioactive material, was from Amersham.

Mutagenesis and Mutant Selection. Random mutant versions of the *Ssadh* gene were obtained by a PCR-mediated strategy according to the method described by Leung et al. (*25*). The oligonucleotides, enzymes, and annealing temperature were the same as described previously (*19*). The amplified DNA was subcloned into pTrc99A and transferred into *E. coli* RB791. Fifty independent clones were grown, and the plasmid was characterized by restriction enzyme analysis. The corresponding protein extracts were prepared from 10 mL culture cells grown and IPTG-induced according to the methods of Cannio et al. (*19*). They were then incubated at 75 °C for 15 min and centrifuged, and the supernatant was assayed for the specific thermophilic ADH activity (*23*). The plasmid DNA isolated from the clone which showed the highest level of thermophilic dehydrogenase activity was sequenced by the dideoxy-chain termination method, using the Sequenase kit and the primers used for the sequencing of the wild type *Ssadh* gene (*19*). The nucleotide sequence was analyzed with the PC gene program obtained from Intelligenetics. The secondary structure from the derived amino acid sequence was predicted using the program Predict (*26*).

Purification of Recombinant Proteins. The recombinant wild type ADH and its mutant were prepared according to the methods of Cannio et al. (*19*) with some modifications. Cells of *E. coli* RB791 harboring the plasmid pTRGSsADH were grown in 2 L of Luria-Bertani medium containing ampicillin (0.1 mg/mL) at 37 °C. At an A_{600nm} of 1.5−1.8, IPTG and $ZnSO_4$ (0.24 g/L and 0.25 mM final concentrations, respectively) were added and the cells were grown overnight (16 h). The cells were harvested by centrifugation, suspended in a 20 mM Tris-HCl buffer (pH 7.4) containing 0.1 mM PMSF, and disrupted by sonication at 4 °C. The lysate was centrifuged, and the supernatant was incubated first in the presence of DNase I (50 μg/mL of solution) and 5 mM $MgCl_2$ for 30 min at 37 °C and then incubated in the presence of protamine sulfate (1 mg/mL of solution) at 4 °C for 30 min. After the nucleic acid fragments were removed by centrifugation, the supernatant was heated at 75 °C for 15 min and the host protein's precipitate was removed by centrifugation. The supernatant was dialyzed against a 20 mM Tris-HCl buffer (pH 8.4) (buffer A) containing 1 mM PMSF and processed on a DEAE-Sepharose Fast Flow column equilibrated in buffer A and developed with a 0 to 0.1 M NaCl gradient. The active pool was concentrated to 1−2 mg of protein/mL by ultrafiltration on a YM 30 Amicon membrane and incubated with α-chymotrypsin (1 mg of protease per 10 mg of protein) for 1 h at 30 °C in the presence of 10 mM 2-mercaptoethanol and 10 mM $CaCl_2$. The digestion products were removed by gel filtration on a Sephadex G 75 column equilibrated in buffer A containing 0.1 M NaCl. The active pool was dialyzed against buffer A, concentrated as described earlier, and stored frozen at −20 °C. No loss of activity was detected in both wild type and mutant enzyme, after several months of storage.

Preparation of Apo ADH. The G 75 gel filtration removed most of the endogenous coenzyme which is strongly bound to the purified wild type ADH (SsADH) as judged by the decrease in the intensity of fluorescence energy transfer band centered at 422 nm and the concomitant increase in the intensity of the main band centered at 319 nm in the emission spectra of the protein excited at 280 nm (see below). The coenzyme-free SsADH was obtained by exhaustive dialysis against buffer A containing 1 μM $ZnCl_2$, until the disappearance of the energy transfer band at 422 nm. The presence of this band is due to the NADH in the wild type enzyme preparation, as the absorption band of the reduced coenzyme partially overlaps the spectrum of protein emission. As an additional test for the presence of NADH, the excitation spectrum was recorded by fixing the emission wavelength at 422 nm. In this case, the presence of the band centered

around 340 nm confirmed the result obtained from the emission spectra. The mutant ADH (mSsADH) was likewise dialyzed, although the poor affinity for the coenzyme (see below) rendered the fluorescence test unsuitable. The apo forms of both ADHs were used throughout this work, when not otherwise specified.

Protein Purity and Mass Analysis. The protein purity was analyzed by SDS−PAGE (*27*) using Coomassie BB G250 or the silver method for staining, and by reverse-phase HPLC, employing a Vidac C4 Chrompack column; protein elution was carried out by mixing 0.1% aqueous TFA with 0.08% TFA in acetonitrile. Samples obtained from the HPLC column were used to determine the molecular mass of the ADH subunit by electrospray mass spectrometry (ES-MS) using a BIO-Q triple-quadrupole mass spectrometer (Micromass). Samples were dissolved in 1% acetic acid in 50% acetonitrile, and 2−10 μL was injected into the mass spectrometer at a flow rate of 10 μL/min. The quadrupole was scanned from *m*/*z* 600 to 1800 at a rate of 10 s/scan, and the spectra were acquired and elaborated using the MassLynx software. Calibration was performed by the multiply charged ions from a separate injection of myoglobin (Sigma; average molecular mass of 16 951.5 Da). All mass values are reported as average masses. Nondenaturing PAGE was carried out according to the Laemmli method with some modifications (*23*).

Enzyme Assay. The activity was assayed toward benzyl alcohol and benzaldehyde as described previously (*23*) with some modifications. The wild type ADH was assayed at 65 °C in 1 mL of standard assay mixture containing 5 mM benzyl alcohol, 3 mM NAD^+, and 0.1 M glycine/NaOH buffer (pH 10.5). The mutant enzyme was assayed under the same conditions, but using 30 mM benzyl alcohol and 25 mM NAD^+. The reverse reaction was assessed in 1 mL of 50 mM Tris-HCl buffer (pH 7.5) containing either 0.2 mM NADH and 0.25 mM benzaldehyde or 0.4 mM NADH and 0.9 mM benzaldehyde for the wild type and mutant ADH, respectively. One enzyme unit represented 1 μmol of NADH produced or utilized per minute at 65 °C on the basis of an absorption coefficient of 6.22 mM^{-1} cm^{-1} for NADH at 340 nm.

Solutions of NAD^+ and NADH were prepared as previously reported (*23*). Kinetic parameter measurements were carried out in duplicate, and kinetic results were analyzed using the program *GraFit* (*28*). Standard errors of the estimated parameters were usually less than 10% of the values.

The concentration of active sites in mSsADH could not be determined by titration with NAD^+ and pyrazole since the enzyme had a low affinity for NAD^+. The turnover numbers of both ADHs are therefore based on the protein concentrations determined by means of the Bio-Rad protein assay kit, and corrections for overestimations of the values were made as previously reported (*23*). The correction factor used resulted in excellent agreement with that calculated by the pyrazole method on SsADH (0.70 and 0.73, respectively).

Effect of pH on Activity. The effect of pH on benzyl alcohol oxidation and benzaldehyde reduction for both ADHs was determined at 65 °C, under the respective standard assay conditions, except that different buffer systems were used (*23*).

Studies with Deuterated Alcohols. The catalytic activity of both the recombinant ADHs on cyclohexanol and benzyl alcohol was measured at 65 °C with saturating concentrations of alcohol and NAD^+, and the V_{max} values were compared to those obtained with the corresponding deuterated alcohols under the same experimental conditions. Each measurement was carried out in triplicate.

Thermophilicity and Thermal Stability. SsADH and mSsADH were assayed in the temperature range of 30−95 °C according to the standard assay conditions using 15 and 3 μg of protein/mL of assay, respectively. The stability at various temperatures was studied by incubating 10 μg/mL protein samples in 0.1 M Tris-HCl (pH 9.0) at temperatures between 30 and 95 °C for 30 min. Each sample was then centrifuged at 5 °C and the residual activity assayed as described earlier. Light scattering was monitored by fluorescence with the same excitation and emission wavelength set at 480 nm, and a 1.5 nm spectral bandwidth.

Thermal Inactivation. SsADH and mSsADH (10 μg/mL) were incubated in 0.1 M Tris-HCl (pH 9.0) at temperatures between 80 and 95 °C. The samples were cool-centrifuged at regular intervals, and the activity was assayed as described earlier. The data were fitted to a single-exponential decay with a rate constant of thermal inactivation k_i, according to

$$\ln(\%\ \text{activity}) = -k_i t$$

The activation energy values (E_a) for the thermal inactivation process were determined with the Arrhenius plot of ln k_i versus the inverse of the absolute temperature (*29*). The activation enthalpy ($\Delta H^{\ddagger}$), activation entropy ($\Delta S^{\ddagger}$), and activation free energy ($\Delta G^{\ddagger}$) for each temperature were calculated according to the equation

$$\Delta H^{\ddagger} = E_a - RT$$

$$\Delta G^{\ddagger} = -RT \ln(k_i h/k_b T)$$

$$\Delta S^{\ddagger} = (\Delta H^{\ddagger} - \Delta G^{\ddagger})/T$$

where k_i is the first-order inactivation rate constant (s^{-1}), k_b is the Boltzmann constant (1.3805×10^{23} J K^{-1}), h is Planck's constant (6.6256×10^{-34} J s), R is the gas constant (8.3144 J K^{-1} mol^{-1}), and T is the absolute temperature (*29*).

Inactivation by Denaturing Agents. The stability of the two ADHs against denaturing agents was determined by assaying the activity in samples incubated for 30 min at 30 °C in the presence of different guanidinium chloride and SDS concentrations. In each case, the protein concentration was 70 μg/mL in 0.1 M Tris-HCl buffer (pH 9.0).

Thermolytic Hydrolysis. SsADH and mSsADH (0.1 mg/mL) were incubated at 50 °C in 0.1 M Tris-HCl (pH 8.5) containing 2 mM $CaCl_2$ in the presence of thermolysin (10:1 ADH:protease mass ratio), and the activity was monitored at defined times.

Fluorescence Studies. Fluorescence protein spectra (λ_{ex} = 280 nm) were recorded at 25 °C with a JASCO FP-777 spectrofluorometer equipped with an external thermostated bath. The dependence of protein fluorescence on pH was studied using 70 μg/mL protein solutions in a 50 mM Tris-HCl buffer with 0.1 M NaCl at different pH values obtained by successively adding a small amount of 5 M NaOH. The coenzyme binding studies with fluorescence quenching were

performed at 25 °C in 50 mM Tris-HCl (pH 8.8), as described previously (*23*).

In addition to enzymatic activity monitoring, the guanidine-dependent equilibrium transitions were monitored by fluorescence (λ_{ex} = 280 nm), by recording the change in fluorescence emission at λ_{em} = 319 and 324 nm for SsADH and mSsADH, respectively.

The interaction of the fluorescent dye 8-anilino-1-naphthalenesulfonic acid (ANS) with the two ADHs was studied by measuring the fluorescence emission of the protein complexed dye upon excitation at 370 nm. The concentration of ANS was determined using a ϵ_{1cm} of 5.7×10^3 M^{-1} cm^{-1} at 360 nm. For our purposes, the absolute quantum yield of the fluorescence of the ANS bound to ADHs was not directly determined. Titrations were performed by adding aliquots of a concentrated ANS solution to 0.2 μM holo- or apoenzymes in 50 mM Tris-HCl (pH 8.8) at 25 °C and measuring the fluorescence at the emission maximum 30 s after mixing. The holo forms were obtained by adding 10 μM and 1 mM NAD^+ to the apo SsADH and mSsADH, respectively. All results were corrected for fluorescence of dye, protein, and reagents. The fluorescence data of mSsADH were corrected for the inner filter effect, according to the procedure of Brand and Witholt (*30*). Binding constants were determined by applying the Scatchard procedure with the program *GraFit* (*28*).

Circular Dichroism Studies. CD data were collected with a JASCO J-710 spectropolarimeter equipped with computer-controlled temperature cuvette holders kept under a constant N_2 flux. Far-UV CD spectra in the 190−250 nm region were recorded with 1.0 mm path length cells containing 71 μg/mL protein in buffer A. The enzyme solution was filtered through a 0.45 μm filter (Millipore) before the measurement was taken. Near-UV CD spectra (240−340 nm) were obtained with a 10 mm cell containing 1.4 mg/mL protein in the same buffer. Final spectra, representing the average of at least five tracings, were corrected for the buffer and free coenzyme spectra. CD analysis was performed by using computer software according to Yang et al. (*31*) to determine the secondary structure of proteins. Since the protein data set of this procedure only contains spectra of mesophilic proteins at room temperature, the computed secondary structure fractions are indicative of the overall structure organization.

Determination of Ammonia. The occurrence of deamidation was investigated by incubating samples of the two enzymes [0.2 mg/mL, in 0.1 M Tris-HCl (pH 9.0)] in sealed ampules at 96 °C for determined periods of time. After cooling and centrifugation, the supernatants were tested for the presence of ammonia by microfluorimetric enzymatic assay (*32*). The electrophoretic analysis of deamidated species was precluded due to the insolubility of the precipitate proteins.

RESULTS

Expression and Location of the Mutation. Analysis of the ADH gene sequence isolated from the *E. coli* clone, which expressed the highest thermophilic and thermoresistant enzyme, revealed only one point mutation (A → T) located at position 1089 of the nucleotide sequence (*18*). This mutation produces the Asn → Tyr replacement. Such a change did not affect the level of gene expression, since optimal conditions for cell growth and induction time were found to be the same for both the recombinant wild type (SsADH) and mutant (mSsADH) enzymes.

Alignment of mSsADH and HLADH sequences with the consensus derived from the alignment of 46 ADHs (*33*) revealed the overall conservation and allowed the localization of the Asn249Tyr position at the coenzyme binding domain on the turn connecting the βD-sheet with the αE-helix in the so-called Rossmann folds (*34*). The turn (see below, highlighted in bold) presents an essentially polar character, which is typical of these secondary structure elements (*35*):

^{244}V I D L **N N S E** K T L S^{255}	SsADH
^{244}V I D L N Y S E K T L S^{255}	mSsADH
^{243}V E C T G N I E A M I S^{254}	consensus sequence (*33*)
^{240}I I A G G N A D I M A T^{251}	TBADH (*18*)

Furthermore, it was observed that asparagines are strong turn formers (*36*), and occur with a significantly higher frequency than other amino acid residues on the N-cap of α-helix (*37*). It is important to note that the alignment reported above indicates that the Asn249 residue is highly conserved.

Secondary structure prediction yielded the following apparent composition of the secondary structure: 26.5 and 27.1% α-helix, 23.3 and 23.4% β-sheet, and 50.1 and 49.6% other (loop) for SsADH and mSsADH, respectively. The number of tyrosine residues rises from 12 to 13 per subunit upon mutation.

Protein Purity and Mass Analysis. The purification procedure yielded 30−50 mg of both recombinant proteins per liter of culture with purities of 95.0 and 99.5% before and after the proteolysis step, respectively, as judged by SDS−PAGE and RP-HPLC analysis. Importantly, the ES-MS analysis revealed no cleavage of the polypeptide chain by the protease treatment of SsADH and its mutant. The molecular masses of the subunit proved to be 37 585.9 ± 5.3 and 37 627.7 ± 2.2 Da for SsADH and mSsADH, respectively, thus agreeing with the data determined by peptide and gene analysis (*18*) and the substitution of an Asn for a Tyr residue.

Optimal pH and Thermophilicity. The specific activity of mSsADH is 26.1 units/mg, whereas that of SsADH is 4.1 units/mg, as determined at 65 °C, using benzyl alcohol as the substrate. Like native SsADH activity (*23*), the wild type ADH activity on benzyl alcohol only showed a slight dependence on pH, with a maximum around 9.0, while the activity of the mutant enzyme depended more closely on pH, with a maximum at about 8.5. The apparent optimal pH for the benzaldehyde reduction ranged from 6.9 to 7.5 for both the enzymes (data not reported).

The effect of temperature on the activity of the recombinant ADHs is shown in Figure 1. The rate of the direct and reverse reaction increases as far as an instrumental limit of 93 °C for both the enzymes, although there is a more marked increase for the mutant ADH. The appearance of the break at about 52 °C for the benzyl alcohol oxidation catalyzed by mSsADH is due to coenzyme depletion. This does not occur for the inverse reaction, where NADH is present in saturating concentrations at elevated temperatures. In Table 1 are listed the thermodynamic activation parameters for the oxidation and reduction reactions of both ADHs calculated

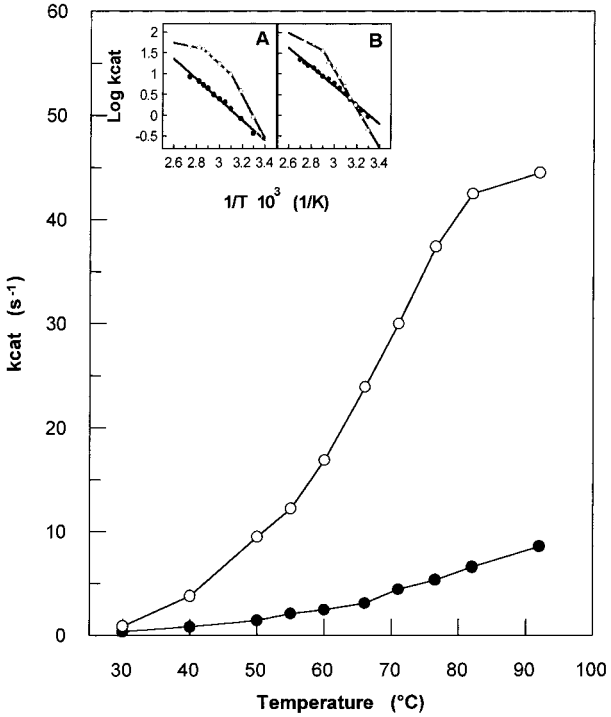

FIGURE 1: Dependence of SsADH (●) and mSsADH (○) activity on temperature. The assays were carried out as described in Materials and Methods, using benzyl alcohol (main plot) as the substrate. Inset A shows the Arrhenius plot of the same data. Inset B shows the Arrhenius plot from the thermophilicity curve (not shown) determined using benzaldehyde as the substrate. The values of the activation energy are 46.7 and 99.1 (first slope) kJ/mol (plot A) and 43.8 and 90.0 kJ/mol (plot B) for SsADH and mSsADH, respectively.

Table 1: Thermodynamic Activation Parameters for SsADH and mSsADH Redox Reaction at 50 °C[a]

enzyme	E_a (kJ mol^{-1})		$\Delta G^{\ddagger}$ (kJ mol^{-1})		$\Delta H^{\ddagger}$ (kJ mol^{-1})		$\Delta S^{\ddagger}$ (kJ mol^{-1} K^{-1})	
SsADH	46.7	43.8	342.1	344.3	44.0	41.1	−0.92	−0.93
mSsADH	99.1[b]	90.0[b]	347.5	345.4	96.4	87.3	−0.77	−0.79

[a] The E_a values are from the Arrhenius plot of Figure 1; the other parameters were calculated according to the relationship reported in Materials and Methods. $\Delta G^{\ddagger}$ was determined from the k_{cat} values measured at 50 °C for benzyl alcohol oxidation (left column) and benzaldehyde reduction (right column). [b] These values refer to the lower-temperature segment of the Arrhenius plots. SD = ± 5% and 2% for E_a and $\Delta G^{\ddagger}$ values, respectively.

from the Arrhenius plots (Figure 1) according to the relationships reported earlier. The k_{cat} values used for the $\Delta G^{\ddagger}$ calculations refer to a representative temperature (50 °C) under the break point observed for the mSsADH oxidation. It is evident that the entropic and enthalpic factors contribute to the energy barrier to reaction ($\Delta G^{\ddagger}$) unlike the case for the wild type enzyme and its mutant.

Kinetic Characterization. A comparison of the steady state kinetic parameters for the wild type and mutant ADH, determined at 65 °C with various substrates, is reported in Table 2. The Asn249Tyr replacement considerably changes the catalytic pattern of the wild type enzyme, affecting both its specificity and efficiency. The affinity of the mutant decreases for all the alcohols and aldehydes tested, as indicated by K_m values, but to a greater extent for the coenzyme (25-fold for NAD^+ and 16-fold for NADH).

Table 2: Kinetic Constants for SsADH and mSsADH[a]

substrate	SsADH k_{cat} (s^{-1})	SsADH K_m (mM)	SsADH k_{cat}/K_m (s^{-1} mM^{-1})	mSsADH k_{cat} (s^{-1})	mSsADH K_m (mM)	mSsADH k_{cat}/K_m (s^{-1} mM^{-1})
1-propanol	2.6	0.6	4.3	16.6[b]	1.70	9.7
cyclohexanol	1.2	0.03	40	15.9[b]	1.9	8.4
benzyl alcohol	3.6	0.26	13.8	21.7[b]	1.5	14.5
4-methoxybenzyl alcohol	3.3	0.23	14.3	25.5[b]	1.24	20.5
NAD^+	3.4	0.5	6.8	50.0	12.4	4.0
benzaldehyde	11.3	0.03	376.0	25.5	0.26	98.0
4-methoxybenz-aldehyde	3.3	0.024	137.0	20.5	0.86	23.8
NADH	10.3	0.013	792	25.3	0.21	120.0

[a] The activity was measured at 65 °C as described in Materials and Methods. Kinetic constants for NAD^+ and NADH were determined with benzyl alcohol and benzaldehyde, respectively. k_{cat} is the turnover number of the forward and reverse reactions. [b] NAD^+ at a nonsaturating concentration of 30 mM.

However, the increase in the K_m of cyclohexanol is even more marked (60-fold). The catalytic rate increased by about 7-fold for the alcohols tested, except for cyclohexanol which is more quickly oxidated by mSsADH than the other alcohols (13-fold), although it is poorly accepted as a substrate. For the reverse reaction, mSsADH also shows increased activity. In fact, 4-methoxybenzaldehyde is 6-fold more quickly reduced, although much less accepted compared to the unsubstituted benzaldehyde. However, the catalytic efficiency does not improve much, whereas the decrease in affinity is large.

With deuterated benzyl alcohol and cyclohexanol as substrates, the V_{max}^{H}/V_{max}^{D} ratio proved to be 1.1 ± 0.1 and 1.2 ± 0.1 for SsADH and 1.5 ± 0.1 and 2.5 ± 0.2 for mSsADH, respectively.

Fluorescence Studies. A comparison of the emission spectra obtained by excitation of SsADH and mSsADH at 280 nm and pH 8.8 in the presence and absence of the reduced coenzyme is presented in Figure 2. The shape of mSsADH spectra (Figure 2A) appears to be similar to that of SsADH (Figure 2B). However, the emission maximum of the mutant enzyme appears 5 nm redder, and the fluorescence intensity is about 25% higher with respect to that of the wild type ADH. Furthermore, the tryptophan fluorescence intensity of the SsADH proves to be 3-fold higher than that of a solution containing the same L-tryptophan equivalents (eight Trp residues per ADH molecule), thus suggesting that the enzyme supports an energy transfer from tyrosyl to tryptophan residues.

Ionization of L-tyrosine produces a weakly fluorescent tyrosinate (*38*), and the pK_a for the ionization of Tyr residues in most proteins usually lies in the range of 9−12 (*39*). Therefore, the fluorescence spectra of SsADH and its mutant were compared at various pHs to detect structural differences in tertiary structure which can be attributed to the additional Tyr249. As expected, the emission intensity of the intrinsic fluorescence of both ADHs decreased as the pH increased, due to the lower degree of energy transfer from tyrosinate to Trp residue(s). Moreover, a shoulder corresponding to the Tyr emission appeared at 303 nm as the pH was increased (data not reported). The emission dependence on pH at 303 nm yields similar pK_a values (10.3 ± 0.1) for both the ADHs (Figure 2, inset). Furthermore, both the proteins showed the

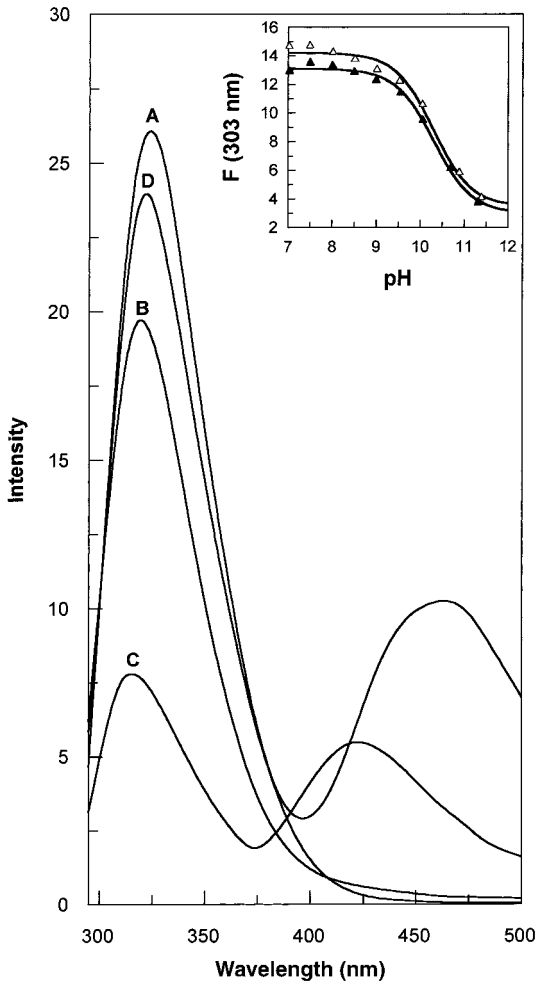

FIGURE 2: Fluorescence spectra of SsADH in the absence (B) and presence (C) of 1 μM NADH and of mSsADH in the absence (A) and presence (D) of 105 μM NADH (λ_{ex} = 280 nm). The enzyme concentration was 1 μM in 50 mM Tris-HCl (pH 8.8). Spectrum D has been corrected for the inner filter effect. In the inset are pH titration curves for the fluorescence intensity at 303 nm of SsADH (▲) and mSsADH (△), as determined in the above buffer containing 0.1 M NaCl. Data points were fitted to an equation describing a single ionization with the program *GraFit* (*28*). Excitation and emission slit bandwidths were 5 nm.

same electrophoretic mobility during nondenaturing PAGE (data not reported). These data suggest that no important change in charge on the SsADH surface occurred upon mutation.

The addition of equimolar amounts of NADH to the apo SsADH resulted in 52% quenching and a wavelength shift of 5 nm in fluorescence emission, while a second peak appeared at about 422 nm due to energy transfer from intrinsic chromophores of the protein to the bound coenzyme (Figure 2C). These effects were not observed for the mSsADH. However, the addition of a 100-fold molar excess of NADH to the apo mSsADH was needed to obtain a 10% quenching level and the appearance of a large band centered at 462 nm, which is due to free NADH emission (Figure 2D). Moreover, when the NAD^+ and NADH were added, even at higher concentrations, no shift in wavelength was observed.

The values of the dissociation constant (K_d) were 0.10 ± 0.02 and 0.02 ± 0.01 μM for NAD^+ and NADH, respectively, as determined by the titration of SsADH at pH 8.8 and 25 °C. The titration data for mSsADH, after correction for the inner filter effect, yielded values for the apparent K_d of 141 ± 7 and 98 ± 5 μM for NAD^+ and NADH, respectively.

CD Data. CD spectra were recorded in the amide and aromatic regions so some secondary structure elements of the protein and the conformational environment of the aromatic residues could be investigated. SsADH and mSsADH showed a CD spectrum typical of α-helical proteins, with double minima at 208 and 220 nm. Moreover, the CD spectra in the range of 220−250 nm overlap, thus excluding aromatic extra contributions by the Tyr249 to the CD signal in the peptide region (*40*) (data not reported). CD analysis yielded the following apparent composition of the secondary structure: 23.8 and 26.5% α-helix, 44.9 and 42.6% β-sheet, 5.4 and 6.8% turn, and 25.8 and 24.0% random for SsADH and mSsADH, respectively.

These data indicate that the Asn249Tyr substitution has slightly changed the helicity and the β-sheet content. However, the α-helix contents are similar to those anticipated by secondary structure analysis. The near-UV CD spectrum reflects changes in the asymmetry of the environment, and these were more pronounced in the 275−282 nm tyrosine range than in phenylalanine and tryptophan ranges of 255−270 and 286−292 nm, respectively (data not shown).

Detection of Surface Hydrophobicity. The fluorescent dye, ANS (*41*), was used as a probe to detect differences in surface hydrophobicity between the two ADHs and conformational changes upon coenzyme binding. When the protein (5 μM) was added to 18 μM ANS, which was excited at 370 nm, a large increase in emission intensity occurred for the mSsADH compared to that for SsADH, in addition to a similar blue shift (55 and 60 nm, respectively) of the emission maximum. The level of fluorescence emission of the ANS−SsADH complex further increased more than 5-fold in the presence of excess coenzyme, accompained by a further blue shift of 30 nm. Instead, the presence of a large excess of NAD^+ slightly affected the ANS binding to the mSsADH molecule and did not induce a further shift of the emission maximum.

Binding studies yielded K_d values of 51 ± 6 and 6 ± 1 μM for apo and holo SsADH and 11 ± 1 and 14 ± 3 μM for apo and holo mSsADH, respectively, which reflect the higher hydrophobicity of the ANS binding site(s) on the mSsADH molecule. The binding analysis points to the stoichiometry of four dye molecules per SsADH and mSsADH tetramer both in the absence and in the presence of coenzyme. This hints that the conformational change induced by the coenzyme has increased the hydrophobicity of the same ANS binding region on the molecule and that the binding sites for the dye and coenzyme molecule are not the same. Inhibition kinetic studies support this observation since ANS does not affect the K_m and V_{max} values of both ADHs (data not shown).

Thermoinactivation of SsADH and mSsADH. Thermal denaturation of the wild type and mutant ADH was monitored by activity and fluorescence emission at 480 nm after incubation for 30 min at different temperatures and a protein concentration of 10 μg/mL (Figure 3). The mutant enzyme seems more thermoresistant than the wild type up to a temperature of 80 °C, after which its activity decreases abruptly, resulting in a transition temperature (3−4 °C) that

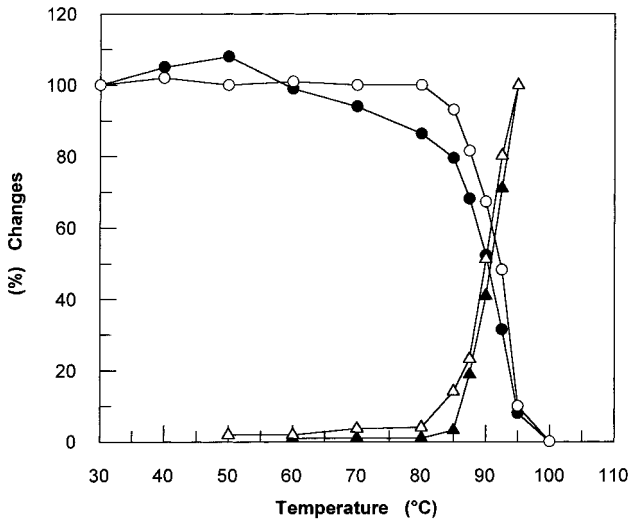

FIGURE 3: Thermal denaturation of SsADH (black symbols) and mSsADH (white symbols) monitored by activity (circles) and fluorescence emission (triangles). λ_{ex} and λ_{em} = 480 nm. The enzyme concentration was 10 μg/mL in 0.1 M Tris-HCl (pH 9.0). Activity measurements were carried out under the conditions of the standard assay. The substrate was benzyl alcohol; the assay temperature was 65 °C.

is higher than that of the wild type enzyme. Furthermore, the midpoint of the SsADH thermal deactivation and aggregation transition coincide, whereas the mSsADH aggregation transition precedes the deactivation by about 1 °C. The aggregation is very marked for the mutant ADH at higher protein concentrations, evidently as a consequence of the more extended hydrophobic surface; in fact, at 70 μg/mL, the aggregation precedes the inactivation of the mutant ADH by about 14 °C, and by only 3 °C that of the wild type (data not reported).

As the apparent transition curves were not used to study the thermodynamics of equilibrium stabilization due to irreversible aggregation accompanying the thermal denaturation, the kinetic thermal stabilities of the two ADHs were investigated. Figure 4 shows the first-order plots for thermal inactivation of both enzymes at a protein concentration of 10 μg/mL in the range of 80−95 °C. The corresponding Arrhenius plots (insets in panels A and B of Figure 4) yield activation energy values of 222 ± 32 and 470 ± 42 kJ/mol for the wild type and mutant ADH, respectively. The values of $\Delta G^{\ddagger}$, $\Delta H^{\ddagger}$, and $\Delta S^{\ddagger}$ calculated at each temperature are summarized in Table 3. $\Delta H^{\ddagger}$ and $\Delta S^{\ddagger}$ values for both enzymes do not change with temperature in the range of 80−95 °C. $\Delta\Delta G^{\ddagger}$ values between the wild type and mutant ADH are maximal at 80 °C, indicating a higher stability of the latter at this temperature. In addition, activation entropy is higher for the mutant than for the wild type ADH by about 700 J mol^{-1} K^{-1}, thus reflecting some loosening of the activated complex or changes in polarity which decrease the level of solvent binding. The marked increase in E_a and, consequently, in activation enthalpy suggests that some intramolecular stabilizing forces could be introduced by the Asn249Tyr substitution. Furthermore, the relatively low E_a value for SsADH seems to suggest that its thermoinactivation is due not only to conformational changes but also to a covalent process (*42*).

Deamidation Reaction. Close inspection of the SsADH amino acid sequence (*18*) reveals that Asn249 has the highest deamidation occurrence rate among the 12 Asn residues present in the polypeptide chain, as it is followed by a Ser residue which is known to increase the deamidation rate (*43*). The replacement of the Asn249 by a Tyr residue leaves the Asn248 residue to precede the aromatic amino acid which is known to correlate with a relatively low deamidation rate (*43*). Therefore, greater ammonia development should be expected to occur from the wild type SsADH, with respect to the mutant enzyme, provided that the thermoinactivation conditions adopted here and structural requirements are favorable to a deamidation reaction (*43*). The fluorescence test for ammonia in the supernatant of thermoinactivated SsADH and mSsADH yielded the data shown in Figure 5, which describes the evolution of ammonia during the incubation of the two enzymes at 96 °C and pH 9.0. The mutant enzyme releases less ammonia than the wild type

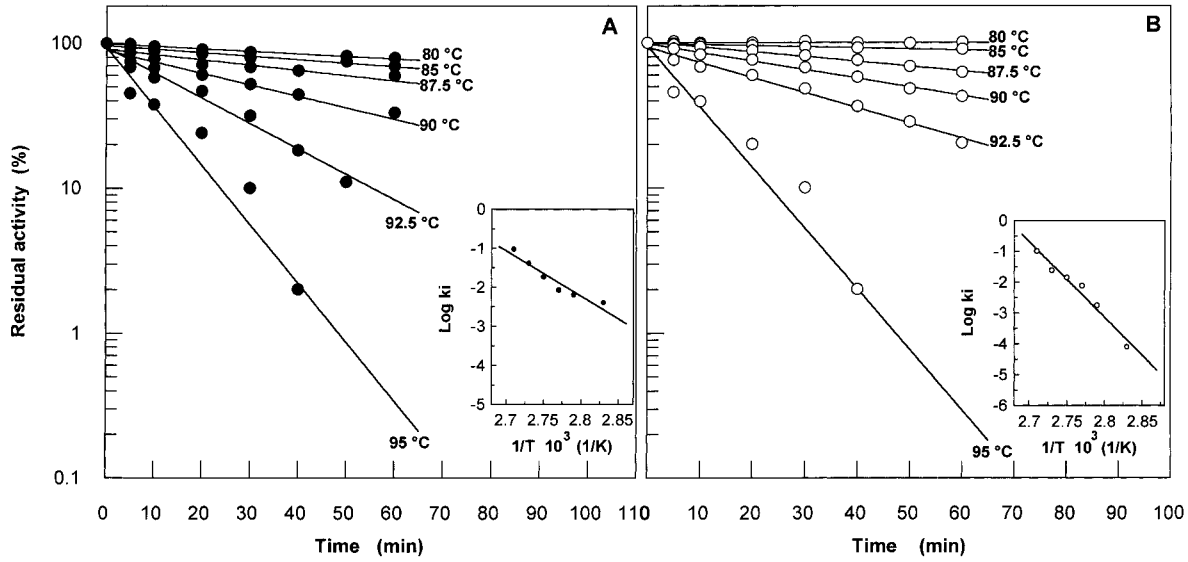

FIGURE 4: First-order plot for thermal inactivation of SsADH (A) and mSsADH (B) determined at different temperatures. The enzymes at a concentration of 10 μg/mL were incubated at the indicated temperatures and assayed as described in the legend of Figure 3. The insets show Arrhenius plots corresponding to thermoinactivation data. To calculate k_i values, experimental data points were computer fitted to an equation describing a single-exponential decay using the program *GraFit* (*28*).

Table 3: Thermodynamic Activation Parameters for Thermal Inactivation of SsADH and mSsADH[a]

enzyme	T (°C)	$\Delta G^{\ddagger}$ (kJ mol^{-1})	$\Delta H^{\ddagger}$ (kJ mol^{-1})	$\Delta S^{\ddagger}$ (kJ mol^{-1} K^{-1})
SsADH	80	426	219	−0.58
	85	431	219	−0.59
	87.5	433	219	−0.59
	90	434	219	−0.59
	92.5	434	219	−0.58
	95	434	219	−0.58
mSsADH	80	437	467	0.08
	85	434	467	0.09
	87.5	433	467	0.09
	90	434	467	0.08
	92.5	436	467	0.08
	95	434	467	0.08

[a] Data are from experiments performed with a 10 μg/mL enzyme concentration, in 0.1 M Tris-HCl (pH 9.0). $\Delta G^{\ddagger}$ values were determined from the first-order rate constants (Figure 4); $\Delta H^{\ddagger}$ values were determined from their temperature dependence (Figure 4, inset), and $\Delta S^{\ddagger}$ values were calculated from $\Delta G^{\ddagger}$ and $\Delta H^{\ddagger}$. SD = ±10%.

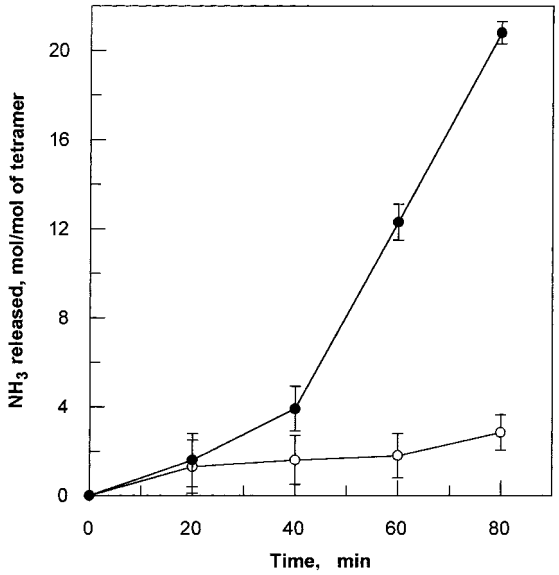

FIGURE 5: Deamidation of amide residues of SsADH (black symbols) and mSsADH (white symbols) on heating at 96 °C. The proteins, 0.21 mg/mL in 0.1 M Tris-HCl (pH 9.0), were incubated in sealad test tubes for various period of time, and the amount of ammonia dissolved in the supernatant was determined enzymatically with glutamate dehydrogenase (*32*).

enzyme upon exposure to high temperature as a consequence of the Asn249Tyr substitution. Moreover, the cooperative behavior of SsADH ammonia evolution indicates that the initial deamidation, which can presumably be ascribed to Asn249, leads to changes in structure and/or partial unfolding which in turn promote further deamidation and degradation of the protein. Therefore, the random deamidation of asparagine (not excluding glutamine) residues occurs on prolonged heating of both enzymes. Furthermore, when half of the enzymatic activity is lost due to thermoinactivation (Figure 4), <1 mol of ammonia per mole of subunit is released from the wild type enzyme, thus suggesting that at least part of the thermal damage associated with inactivation can be attributed to deamidation.

Evidence that structural zinc-depleted SsADH loses its thermal resistance (*17*, *18*) points to the relaxation of the structural zinc bonds as a cause of SsADH thermoinactivation. Thus, the thermal kinetic activity of both the ADHs

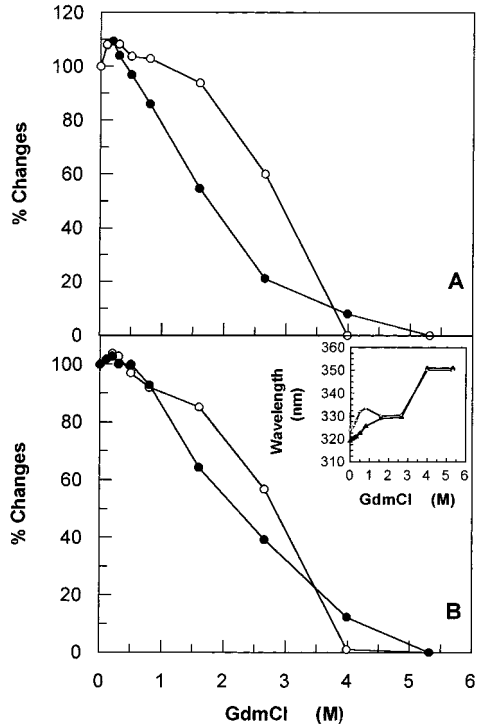

FIGURE 6: GdmCl-dependent unfolding transitions of SsADH (A) and mSsADH (B) monitored by activity (●) and fluorescence (○). The enzyme concentration and activity assay were like those described in the legend of Figure 3. Fluorescence emission was registered at 319 (A) and 324 nm (B); λ_{ex} = 280 nm. In the inset is shown the GdmCl dependency of the emission fluorescence spectral position of SsADH (▲) and mSsADH (△); the wavelength corresponding to the maximum of each spectra is reported vs the denaturant concentration. The plot is representative of two independent determinations (SD = ±0.5 nm).

was studied in the absence and presence of metal-chelating agents, such as EDTA and *o*-phenanthroline. Both the enzymes turned out to be quite stable at 70 °C and at a concentration of 35 μg/mL in the absence of the chelating agents. Their addition, at millimolar concentrations, to the incubation mixtures caused the 30% drop in SsADH activity and no effect on that of mSsADH.

Stability in the Presence of Denaturing Agents. The denaturation transitions for SsADH and mSsADH induced by GdmCl and monitored by activity and fluorescence are shown in Figure 6. The $c_{1/2}$ values, i.e., the denaturant concentration needed to cause 50% inactivation, are 1.7 and 2.2 M GdmCl for the wild type and mutant ADH, respectively. However, the denaturation profiles show that SsADH is slightly more resistant than its mutant up to a chaotropic agent concentration of 1 M. Interestingly, the emitting chromophores in the mSsADH molecule appear to regain some of their hydrophobic environment between 1 and 1.5 M denaturant, after which their solvent exposure parallels that of the wild type enzyme chromophores (Figure 6B, inset). The emission spectra of the totally inactive enzymes reveal the disappearance of the single peak at 319 and 324 nm, which is substituted by a band centered at 305−308 nm that is typical of tyrosine emission, and another centered at 351 nm, which is characteristic of tryptophan that is completely exposed to the solvent (data not reported). It is important to note that the wild type ADH activity increases at low denaturant concentrations whereas the mutant enzyme is activated very little.

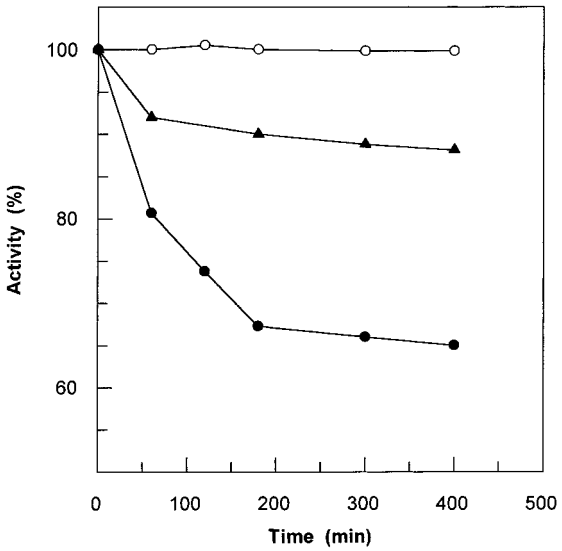

FIGURE 7: Effect of thermolysin on the SsADH (●) and mSsADH (○) activities. The enzymes, 0.1 mg/mL in 0.1 M Tris-HCl (pH 8.5) containing 2 mM $CaCl_2$, were incubated at 50 °C in the presence of thermolysin (10:1 ADH:protease mass ratio), and their activity was assayed at defined times. SsADH was also incubated as described above but in the presence of a 10-fold molar excess of zinc chloride with respect to thermolysin (▲).

SDS-induced equilibrium transition curves for SsADH and mSsADH proved to be similar, with the $c_{1/2}$ value around 0.13% SDS, after incubation for 60 min at 30 °C. Moderate surfactant concentrations (0.05% SDS) only activated the wild type enzyme (by 115%) but not the mutant enzyme (data not shown). Furthermore, SsADH at 70 μg/mL in 0.1 M Tris-HCl (pH 9.0) was activated up to 150%, after incubation for 48 h at 30 °C. However, holo SsADH and holo and apo mutant ADH retained 100% of the initial activity under the same experimental conditions.

Thermolytic Hydrolysis. The above results suggested that some tightening of the overall structure of SsADH occurred upon Asn248Tyr substitution. The alternative hypothesis was that the mutant molecule was not activated further as it was already endowed with intrinsic flexibility at the catalytic site, and this contrasts with the higher $c_{1/2}$ value observed for the deactivation of mSsADH by GdmCl. The lack of proteolytic cleavage observed after the α-chymotrypsin step adds further evidence that the mutant protein apparently conserves the structural integrity of the wild type ADH, but this evidence is limited to the protease specificity and moderate conditions reaction.

Thus, proteolysis experiments at a temperature higher than 30 °C using a different protease were performed to verify the latter hypothesis. The protease chosen was thermolysin, since it is active within a broad range of temperatures (*44*). Figure 7 shows the effect of the incubation with large amounts of thermolysin on the enzymatic activity of both SsADH and mSsADH. The first loses more than 30% of its activity after 3 h at 50 °C, whereas the mutant enzyme retains 100% of its activity even after longer exposure. The level of inactivation of SsADH is lower in the presence of added zinc ions (Figure 7, middle curve), which is consistent with the observed inhibition of thermolysin by an excess of zinc ions (*45*). Therefore, the second slow phase of SsADH inactivation could reflect some inactivation of the protease due to the zinc released as a result of SsADH digestion, but the possibility that it represents the residual activity resulting from limited proteolysis has not been excluded.

DISCUSSION

Random mutagenesis by error-prone PCR and a screening method based on heat resistance and thermophilicity tests proved to be a successful strategy for isolating a mutant of the archaeal ADH endowed with increased activity, and improved thermal resistance with respect to the native enzyme.

The Asn249Tyr substitution alters the environment of both the coenzyme- and substrate-binding site. The K_d values for NAD^+ and NADH increase by 3 orders of magnitude, and this change in coenzyme affinity is higher than that observed in the native SsADH following Cys38 carboxymethylation (*23*). In this case, the negatively charged carboxymethyl group was presumed to repel the pyrophosphate moiety of the coenzyme, thus causing the K_d for the NADH−enzyme complex to increase by 2 orders of magnitude. Presumably, the Tyr249 sterically and electrostatically contrasts the interaction of the coenzyme molecule with the binding site. However, the substrate binding is also substantially affected by the substitution. In fact, the large decreases in the cyclohexanol and 4-methoxybenzaldehyde affinities suggest that the bulky phenolic group sterically disturbs the interactions at the substrate binding pocket.

The increased catalytic activity of the mutant enzyme is due to the faster release of the coenzyme as a direct consequence of the major weakening of the binary complex. Accordingly, the kinetic isotope effect studies show that the NADH release is rate-limiting for the recombinant SsADH as observed for the native enzyme (*23*), but that the hydride transfer step partially controls the overall reaction catalyzed by the mutant enzyme.

The activation of mSsADH and Cys38-modified SsADH (*23*) as well as HLADH mutated at the adenosine moiety binding site (*16*) or modified at essential amino groups (*46*, *47*) suggests a common criterion as a guide for enhancing the turnover of this class of enzymes, namely, to facilitate the coenzyme release by chemical modification or substitutions which are able to electrostatically and/or sterically disturb the coenzyme−enzyme interaction.

The tertiary structure of the wild type ADH is not changed substantially upon the mutation as the fluorescence studies show. The enhancement in intrinsic fluorescence emission can be attributed to the additional tyrosine, presumably located in a position which is favorable for energy transfer to the nearby tryptophan residue. However, a decrease in the rates of relaxation processes, to which the quantum yield is sensitive, cannot be totally excluded (*48*). The similarity in pK_a observed by fluorescence titration indicates that the nearest environment experienced by the tyrosine introduced is not directly exposed to medium.

Previous investigations with HLADH established that protein conformational changes and radiation-less energy transfer processes cause the quenching of protein fluorescence on NADH binding and that NAD^+ quenches essentially by conformational changes (*49*, *50*). A blue shift phenomenon and the appearance of the energy transfer band point to the above quenching mechanism in native (*23*) and recombinant SsADH. On the other hand, both NAD^+ and

NADH quench the fluorescence emission of the mutant SsADH without any shift and energy transfer, suggesting that only small conformational changes affect the protein emission. The absence of an energy transfer process in mSsADH, which is so large in the SsADH, can be due to an unfavorable orientation of the NADH molecule for energy transfer and/or to a slight increase of the donor−acceptor distance. Furthermore, NADH fluorescence is enhanced and its emission maximum blue shifted on binding to SsADH, but in the presence of mSsADH it does not change. This drastic decrease in the relative quantum yield of the flexible NADH molecule may be due to the increased number of deactivating collisions with solvent molecules as well as to limited possibilities for internal conversion as a consequence of a reduced number of points of attachment to some elements of the coenzyme binding structure (*51*).

On the other hand, the mutant enzyme binds the fluorescent probe, ANS, very strongly presumably at the same sites present on the wild type enzyme. A decrease in solvent polarity and, to some extent, an increase in rigidity of the local environment have been demonstrated to increase the quantum yield and decrease the wavelength of emission of amino-substituted naphthalene derivatives (*41*, *48*). However, there is indirect evidence that the region which accepts the ANS molecule on both the ADHs is prevalently hydrophobic in nature. SsADH at a relatively high concentration precipitates in the presence of coenzyme, at room temperature, and the apo form of mSsADH gives a faint precipitate at relatively low concentrations and elevated temperatures.

The substitution at the coenzyme binding domain of the Asn249 with a tyrosine residue has affected not only the catalysis mechanism but also the structural stability of the archaeal ADH, improving its resistance to heat, denaturants, and proteases, without dramatic changes in the overall structure. The lack of the three-dimensional structure makes it difficult to develop an explanation for the stabilization mechanism from a molecular point of view. However, it is evident that the Asn249 plays an important role in the mechanism of irreversible thermal denaturation of SsADH, and that its substitution with a non-heat degradation susceptible residue has produced not only the effect of reducing the deamidation process but also the effect of increasing the rigidity of the molecular edifice.

A plausible hypothesis concerning the latter point is that the Tyr residue, which is more bulky and less polar than the Asn residue, may have occupied the cavity left by the latter, fitting more tightly than the parent residue. The tightening of residues in cavities has been correlated with stabilization (*52*). For example, the role of Asp80Tyr substitution in stabilizing kanamicin nucleotidyltransferase has been found to be correlated with the hydrophobicity of the residue in the protein interior (*53*). It is likely that the interactions of the Asn249 side chain with the environment have been substituted by others, which are more hydrophobic in nature, without excluding the participation of the phenolic OH in specific hydrogen bonding. Furthermore, aromatic−aromatic interactions, hydrogen bonding formation, and packing efficiency have been taken into consideration to explain the correlation between thermostability and the statistical increase in residency in α-helices of tyrosine, glycine, and glutamine residues in thermophilic proteins (*54*).

Although the increase in helicity for mSsADH is slight and depends on the limiting sensitivity of the CD measurement and evaluation errors (*55*), it could also be linked to the observed thermostabilization. Moreover, the possibility of interaction of charged Tyr249 with the αE-helix dipole cannot be excluded.

The coincidence of the fluorescence transitions for both the ADHs and the shift of the guanidine-dependent deactivation for the mutant enzyme to higher denaturant concentrations (Figure 6) suggest some stabilization related to catalysis, and this most likely involves the coenzyme binding domain. Such stabilization seems to be more electrostatic than hydrophobic in nature, as the denaturation transitions by SDS of both the enzymes are coincident.

Proteolysis experiments highlight two important features, namely, the highly limited susceptibility of SsADH to proteolysis, which reflects the considerable structural rigidity achieved by this archaeal protein for functioning at elevated temperatures, and the further tightening of the overall structure induced by the mutation. In addition, α-chymotrypsin, which is endowed with different substrate specificity, is not active on mSsADH. Therefore, it is the decreased flexibility rather than the changes in loop exposure which determines the increased protease resistance shown by the mutant enzyme. In fact, protein thermostability has been correlated to both rigidity and resistance to proteolysis (*53*, *56*).

Data from thermoinactivation performed in the absence and presence of chelating agents add further evidence that the structural tightening achieved by the mutant ADH extends to the whole molecule, and is not limited to specific regions.

The loss of structural zinc and the retaining of catalytic zinc in SsADH on dialysis against chelating agents have been shown by metal analysis (*17*, *18*). The removal of zinc from yeast ADH by DTT or EDTA results in a highly heat-sensitive enzyme; in particular, the temperature dependence of the EDTA effect suggests that some unfolding is necessary to facilitate the accessibility to the chelating molecule (*57*). Furthermore, the removal of the noncatalytic zinc from HLADH is stimulated by raising the temperature, as was proven by the gel filtration technique (*58*).

Consequently, the strong point of the thermal resistance of this archaeal ADH is the tightening of the structural zinc and thus of the loop where the metal is complexed by the Cys100, -103, and -111 and Glu97 residues (*18*). Interestingly, the latter was replaced by a cysteine residue (*33*) to restore the four canonical cysteines that contribute to the structural zinc-binding motif present in all other ADHs (*59*). The Glu97Cys mutant proved to be equally active but less thermostable than native SsADH, showing that at least part of the SsADH thermostability is due to the presence of the glutamate in its structural metal binding site. It is evident that the replacement of Cys with Glu represents a significant achievement in the evolutionary adaptation of SsADH to thermophilic conditions. In this context, it is tempting to speculate that Asn249 deamidation plays a role in timing the degradation of protein in vivo. The high level of conservation of this residue may provide a starting point for verifying this intriguing hypothesis. However, to our knowledge, this is the first evidence of thermoinactivation depending on asparagine deamidation for archaeal enzymes.

As far as the influence of Asn249Tyr substitution on the zinc tightening is concerned, we hypothesize that long-range effects are involved, presumably across hydrogen bond networks or electrostatically through space within the protein scaffolding. It has been suggested (*60*) that making a protein surface more negatively charged results in a stronger metal-binding site. Fluorescence and electrophoresis data indicate no apparent change in the charge on the mSsADH surface with respect to the wild type enzyme. Therefore, it is not unreasonable to assume that the strengthening of structural zinc binding in mSsADH is mainly related to hydrogen bond networks involving the metal ligands, and that such interactions contribute greatly to the increased activation enthalpy associated with the thermoinactivation of the mutant enzyme. This large increase in enthalpy is, however, compensated by an entropy gain, thus resulting in a free energy value which is somewhat higher in the mutant compared to that in the wild type enzyme. In this context, it is evident that the mutation has increased the kinetic thermal stability of SsADH by raising the activation barrier against thermal unfolding.

Changes in relative enthalpic and entropic contributions to activation free energy ($\Delta G^{\ddagger}$) also characterize the energetics of the redox reaction catalyzed by both enzymes (Table 1). The large enthalpy of mSsADH renders its turnover more temperature-dependent, as the thermophilicity curve shows, while the entropy gain indicates that either less solvation accompanies the activated complex formation or the enzyme molecule assumes a somewhat less tight conformation in forming the ternary complex with respect to the wild type enzyme (*34*). However, caution should be used in making this observation because the general catalysis of ADHs follows a multistep mechanism and also because the step which controls the k_{cat} is different in both ADHs. Noteworthy, for SsADH the energy barrier to thermoinactivation is higher than that required for catalysis, which is an essential requisite for enzymes to reach their temperature optimum, and this also applies to mSsADH.

To function optimally at elevated temperatures, SsADH has achieved a proper balance of rigidity and flexibility, which is compatible with stability requirements. A single semiconservative substitution at the coenzyme binding domain has shifted this balance slightly toward the former, resulting in greater thermal resistance without any detriment to the specific activity of the enzyme, which in fact proves to be more active.

This study serves as a good example of how it is possible to improve both the stability and activity of a protein, even with the same substitution.

ACKNOWLEDGMENT

We thank Dr. G. Manco for the analysis of secondary structure prediction and Prof. P. Pucci for the ES-MS analysis.

REFERENCES

1. Brock, T. D. (1986) *Thermophiles, General, Molecular, and Applied Microbiology*, John Wiley and Sons, New York.
2. Somero, G. N. (1996) *News Physiol. Sci. 11*, 72−77.
3. Vihinen, M. (1987) *Protein Eng. 1*, 477−480.
4. Jaenicke, R. (1991) *Eur. J. Biochem. 202*, 715−728.
5. Danson, M. J., Hough, D. W., Russell, R. J. M., Garry, L. T., and Pearl, L. (1996) *Protein Eng. 9*, 629−630.
6. Menendez-Arias, L., and Argos, P. (1989) *J. Mol. Biol. 206*, 397−406.
7. Querol, E., Perez-Pons, J. A., and Mozo-Villarias, A. (1996) *Protein Eng. 9*, 265−271.
8. Shaw, A., and Bott, R. (1996) *Curr. Opin. Struct. Biol. 6*, 546−550.
9. Evans, C. T., Kurz, L. C., Remington, S. J., and Srere, P. A. (1996) *Biochemistry 35*, 10661−10672.
10. Fierobe, H. P., Stoffer, B. B., Frandsen, T. P., and Svensson, B. (1996) *Biochemistry 35*, 8696−8704.
11. Narinx, E., Baise, E., and Gerday, C. (1997) *Protein Eng. 10*, 1271−1279.
12. Arnold, F. H., and Moore, J. C. (1997) *Adv. Biochem. Eng. Biotechnol. 58*, 1−14.
13. Rajalakshmi, N., and Sundaram, P. V. (1995) *Protein Eng. 8*, 1039−1047.
14. Zhou, H.-X., Wong, K.-Y., and Vijayakumar, M. (1997) *Proc. Natl. Acad. Sci. U.S.A. 94*, 12372−12377.
15. Plapp, B. V., Green, D. W., Sun, H.-W., Park, D.-H., and Kim, K. (1993) in *Enzymology and Molecular Biology of Carbonyl Metabolism* (Weiner, H., Ed.) Vol. 4, pp 391−400, Plenum Press, New York.
16. Fan, F., and Plapp, B. V. (1995) *Biochemistry 34*, 4709−4713.
17. Raia, C. A., D'Auria, S., and Rossi, M. (1994) *Biocatalysis 11*, 143−150.
18. Ammendola, S., Raia, C. A., Caruso, C., Camardella, L., D'Auria, S., De Rosa, M., and Rossi, M. (1992) *Biochemistry 31*, 12514−12523.
19. Cannio, R., Fiorentino, G., Carpinelli, P., Rossi, M., and Bartolucci, S. (1996) *J. Bacteriol. 178*, 301−305.
20. Pearl, H. L., Demasi, D., Hemmings, A. M., Sica, F., Mazzarella, L., Raia, C. A., D'Auria, S., and Rossi, M. (1993) *J. Mol. Biol. 229*, 782−784.
21. Esposito, L., Sica, F., Sorrentino, G., Berisio, R., Carotenuto, L., Giordano, A., Raia, C. A., Rossi, M., Lamzin, V. S., Wilson, K. S., and Zagari, A. (1998) *Acta Crystallogr. D54*, 386−390.
22. Cannio, R., Rossi, M., and Bartolucci, S. (1994) *Eur. J. Biochem. 222*, 345−352.
23. Raia, C. A., Caruso, C., Marino, M., Vespa, N., and Rossi, M. (1996) *Biochemistry 35*, 638−647.
24. Brent, R., and Ptashne, M. (1981) *Proc. Natl. Acad. Sci. U.S.A. 78*, 4204−4208.
25. Leung, D. W., Chen, E., and Goeddel, D. V. (1989) *Technique 1*, 11−15.
26. Rost, B. (1997) EMBL Internet Site, Heidelberg, Germany.
27. Laemmli, U. K. (1970) *Nature 227*, 680−685.
28. Leatherbarrow, R. J. (1992) *GraFit*, version 3.0, Erithacus Software Ltd., Staines, U.K.
29. Huang, R. (1981) in *Physical Chemistry with Applications to Biological Systems*, pp 348−389, Mcmillan Publishing Co., New York.
30. Brand, L., and Witholt, B. (1967) *Methods Enzymol. 11*, 776−856.
31. Yang, J. T., Wu, C. S. C., and Martinez, H. M. (1986) *Methods Enzymol. 130*, 208−269.
32. Nazar, B. L., and Schoolwerth, A. C. (1979) *Anal. Biochem. 95*, 507−511.
33. Ammendola, S., Raucci, G., Incani, O., Mele, A., Tramontano, A., and Wallace, A. (1995) *Protein Eng. 8*, 31−37.
34. Eklund, H., Samama, J.-P., and Jones, T. A. (1984) *Biochemistry 23*, 5982−5996.
35. Rose, G. D., Gierasch, L. M., and Smith, J. A. (1985) *Adv. Protein Chem. 37*, 1−97.
36. Chou, P. Y., and Fasman, G. D. (1978) *Annu. Rev. Biochem. 47*, 251−276.
37. Richardson, J. S., and Richardson, D. C. (1988) *Science 240*, 1648−1652.
38. Eisinger, J., Feuer, B., and Lamola, A. A. (1969) *Biochemistry 8*, 3908−3915.
39. Tanford, C. (1962) *Adv. Protein Chem. 17*, 69−105.
40. Woody, R. W. (1978) *Biopolymers 17*, 1451−1467.
41. Brand, L., and Gohlke, J. R. (1972) *Annu. Rev. Biochm. 41*, 843−864.

42. Mozhaev, V. V. (1993) *Trends Biotechnol. 11*, 88−94.
43. Wright, H. T. (1991) *Crit. Rev. Biochem. Mol. Biol. 26*, 1−52.
44. Heinrikson, R. L. (1977) *Methods Enzymol. 47*, 175−189.
45. Holmquist, B., and Vallee, B. L. (1974) *J. Biol. Chem. 249*, 4601−4607.
46. Plapp, B. V., Brooks, R. L., and Shore, J. D. (1973) *J. Biol. Chem. 248*, 3470−3475.
47. Plapp, B. V., Sogin, D. C., Dworschack, R. T., Bohlken, D. P., and Woenckhaus, C. (1986) *Biochemistry 25*, 5396−5402.
48. Stryer, L. (1968) *Science 162*, 526−533.
49. Abdallah, M. A., Biellmann, J.-F., Wiget, P., Joppich-Kuhn, R., and Luisi, P. L. (1978) *Eur. J. Biochem. 89*, 397−405.
50. Laws, W. R., and Shore, J. D. (1979) *J. Biol. Chem. 254*, 2582−2584.
51. Schauerte, J. A., Schlyer, B. D., Steel, D. G., and Gafni, A. (1995) *Proc. Natl. Acad. Sci. U.S.A. 92*, 569−573.
52. Pace, C. N. (1992) *J. Mol. Biol. 226*, 29−35.
53. Matsumura, M., Yahanda, S., Yasumura, S., Yutani, K., and Aiba, S. (1988) *Eur. J. Biochem. 171*, 715−720.
54. Warren, G. L., and Petsko, G. A. (1995) *Protein Eng. 8*, 905−913.
55. Chakrabartty, A., Kortemme, T., Padmanabhan, S., and Baldwin, R. L. (1993) *Biochemistry 32*, 5560−5565.
56. Fontana, A., Fassina, G., Vita, C., Dalzoppo, D., Zamai, M., and Zambonin, M. (1986) *Biochemistry 25*, 1847−1851.
57. Magonet, E., Hayen, P., Delforge, D., Delaive, E., and Remacle, J. (1992) *Biochem. J. 287*, 361−365.
58. Maret, W., Andersson, I., Dietrich, H., Schneider-Bernlöhr, H., Einarsson, R., and Zeppezauer, M. (1979) *Eur. J. Biochem. 98*, 501−512.
59. Vallee, B. L., and Auld, D. S. (1990) *Biochemistry 29*, 5647−5659.
60. Christianson, D. W. (1991) *Adv. Protein Chem. 42*, 281−355.

BI982326E